Water Science & Technology

Water Science & Technology Vol 85 No 9, 2525 doi: 10.2166/wst.2022.132

Phosphorus recovery from a pilot-scale grate furnace: influencing factors beyond wet chemical leaching conditions

G. Boniardi[a], A. Turolla[a,*], L. Fiameni[b], E. Gelmi[a], E. Bontempi[b] and R. Canziani[a]

[a] Department of Civil and Environmental Engineering (DICA), Politecnico di Milano, Piazza Leonardo da Vinci 21, 20133, Milano, Italy
[b] INSTM and University of Brescia, Via Branze 38, 25123, Brescia, Italy
*Corresponding author. E-mail: andrea.turolla@polimi.it

AT, 0000-0002-2902-5004

ABSTRACT

Phosphorus is a non-renewable resource going to be exhausted in the future. Sewage sludge ash is a promising secondary raw material due to its high phosphorus content. In this work, the distribution of 19 elements in bottom and cyclone ashes from pilot-scale grate furnace have been monitored to determine the suitability for the phosphorus acid extraction. Moreover, the influence of some parameters beyond wet chemical leaching conditions were investigated. Experimental results showed that bottom ash presented lower contamination in comparison to cyclone ash and low co-dissolution of heavy metals (especially Cr, Pb and Ni), while high phosphorus extraction efficiencies (76–86%) were achieved. High Al content in the bottom ash (9.4%) negatively affected the phosphorus extraction efficiency as well as loss on ignition, while the particle size reduction was necessary for ensuring a suitable contact surface. The typology of precipitating agents did not strongly affect the phosphorus precipitation, while pH was the key parameter. At pH 3.5–5, phosphorus precipitation efficiencies higher than 90% were achieved, with a mean phosphorus content in the recovered material equal to 16–17%, comparable to commercial fertilizers. Instead, the co-precipitation of Fe and Al had a detrimental effect on the recovered material, indicating the need for additional treatments.

Key words: grate furnace, heavy metals contamination, phosphorus recovery, resource recovery, sewage sludge ash, wet chemical extraction and precipitation

HIGHLIGHTS

- Bottom ashes from pilot-scale grate furnace were suitable for phosphorus extraction.
- Influence of parameters beyond chemical extraction conditions were investigated.
- Al content and particle size significantly influenced phosphorus extraction efficiency.
- pH was the most relevant precipitation parameter unlike the type of precipitating agent.
- pH between 3.5 and 5 led to high phosphorus content in the recovered product.

GRAPHICAL ABSTRACT

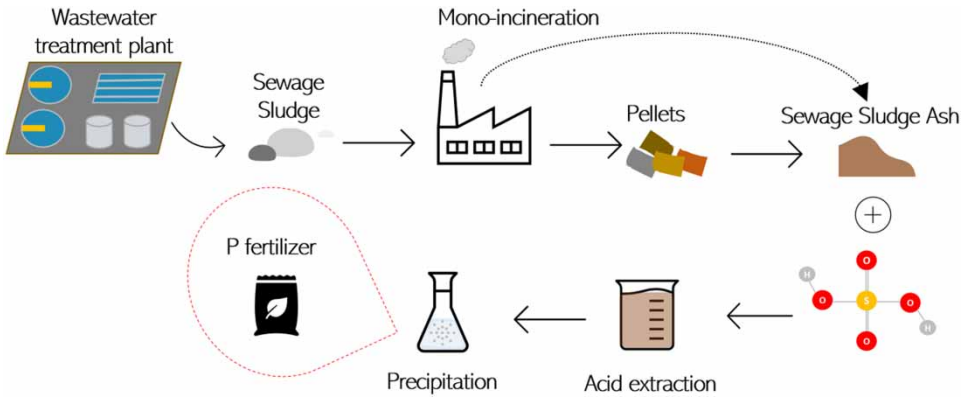

1. INTRODUCTION

Phosphorus is a vital nutrient for all living organisms, including human beings, animals, and crops. It is an irreplaceable and non-renewable resource commonly extracted from natural phosphate rocks. Due to its increasing consumption, mostly attributed to fertilizer manufacturing, phosphate rocks have been introduced in the list of critical raw materials by the European Commission (EC 2017). The global population growth, intensive farming methods and changes in diet in developing countries will accelerate the depletion of ore sources, which is expected in 100–400 years (Desmidt *et al.* 2015). At the same time, the low utilization efficiency of phosphorus in agriculture (below 20%) causes eutrophication, impacting the quality of surface water bodies (Li *et al.* 2019a). Nowadays, the exploration of alternative sources to decrease the pressure on phosphate rocks and to minimise the environmental impact is of paramount importance.

Phosphorus is available in the sewage sludge, in which 80–90% of the discharged phosphorus concentrates during wastewater treatment (Lee & Kim 2017). Moreover, the concerns related to sewage sludge application in agriculture, mostly due to the high heavy metals content, favoured other options for sludge management and disposal such as the mono-incineration. The produced sewage sludge ash comes as enriched phosphorus source, with a mean phosphorus content of 5–11% w/w (Ottosen *et al.* 2013), which is comparable to the content in medium ore grade. According to Donatello & Cheeseman (2013), about 1.7 million tonnes of ashes are produced worldwide every year, and the majority is subsequently landfilled.

During the last few years, in the view of circular economy and a zero-waste approach, more than 30 technological solutions for phosphorus recovery have been developed, among which the wet chemical extraction from sewage sludge ashes has proven to be one of the most effective (Fahimi *et al.* 2021). Its simple setup, low energy consumption and applicability at large scale are the main advantages (Fang *et al.* 2020). Few technological solutions have been scaled-up so far: the available ones at full-scale in Europe are Remondis Tetraphos, Phos4life and EcoPhos processes (Chrispim *et al.* 2019; Fang *et al.* 2020). Beyond high operating costs, the main reasons making technology development and scale-up challenging are related to variations in phosphorus concentration in the sewage sludge ash and recovered product contamination (e.g., by heavy metals) (Li *et al.* 2019b).

Looking at the related literature, due to the maturity of fluidized bed technology, the majority of the studies published refer to wet chemical extraction from fly ash, while very few studies focused on the ashes obtained from grate furnaces (Cheng *et al.* 2020; Fang *et al.* 2020). Data about the mean composition of sewage sludge ashes specifically used for phosphorus extraction is provided in Table S1, in which the type of incineration technology is also considered. As pointed out by Gorazda *et al.* (2007), the incineration technology plays an important role since operating parameters (such as the temperature) and the conditions of each thermal process significantly affect the physical and chemical properties of the ashes produced. From 72 samples collected, only 6% referred to grate furnace, while 68% were derived from fluidized bed incinerators. For 17% of samples, the type of combustion technology was not provided nor easily available. Cheng *et al.* (2020) highlighted that most studies focused on the fluidized bed incinerators with limited insights into the behaviours of heavy metals/metalloids during step grate incineration. For these reasons, we decided to investigate the phosphorus recovery from bottom ashes, which are less enriched with heavy metals compared to fly ashes. The application of grate furnaces can become widespread

in the following years (at least in some areas) since critical raw material recovery from ashes has recently gained much more attention than in the past. In addition, the simplification and reduction of the flue gas line and treatment provided by this kind of technology can promote its diffusion.

Furthermore, most of the previous research efforts addressed the influence of extraction conditions (e.g, acid type, acid concentration, liquid-to-solid ratio, contact time, temperature) on the phosphorus extraction efficiency (PEE), while less attention was posed on the influence of upstream treatments on the downstream phosphorus recovery (Liu *et al.* 2021).

Overall, the type of extractants tested for the leaching process were inorganic acids (H_2SO_4, HCl, HNO_3), organic acids ($H_2C_2O_4$, $C_6H_8O_7$), chelating agents (EDTMP, EDTA) and bases (e.g., NaOH). The highest phosphorus extraction efficiencies (70–100%) were obtained by acids, while bases and complexing agents led to lower extraction efficiencies (9–40%). In general, strong acids can extract phosphorus by breaking the metal-phosphorus bonds, inevitably causing the co-dissolution of unwanted elements such as heavy metals. In literature, to lower the heavy metal content in the recovered material and thus to increase its quality, three main strategies have been considered so far. The first one deals with prevention from leachate contamination, the second one with leachate purification, while the third one is focused on the optimisation of selective precipitation conditions.

Fang *et al.* (2018) investigated the first strategy by introducing a pre-treatment of sewage sludge ash with EDTA (0.02 mol/L) followed by extraction with sulfuric acid (0.2 mol/L). However, even if the purity of the extract was increased, the phosphorus content in the leachate decreased by 29%. Then, the first attempts at leachate purification were made by ion exchange resins (Franz 2008; Xu *et al.* 2012; Wang *et al.* 2018), adsorbent materials (Biswas *et al.* 2009; Yu *et al.* 2021), nanofiltration (Niewersch *et al.* 2014) and liquid-liquid extraction (Hong *et al.* 2005; Baldi *et al.* 2021). Considering the recent literature, Yu *et al.* (2021) proposed the use of a phosphorus selective adsorbent (based on zirconium) to recover 70% of phosphorus in ash as hydroxyapatite, while Baldi *et al.* (2021) found to be effective keeping in contact the acid leachate with an organic solvent solution (isoamyl alcohol) with a ratio of 1:1. They indeed found a phosphorus extraction rate of 81% with low amount of iron and aluminium (extraction rate of 25% and 10%, respectively). Looking at industrial scale, ion-exchange and selective nanofiltration are the actual techniques adopted (e.g., Remondi Tetraphos and EcoPhos), but alternatives to lower the costs are required (Baldi *et al.* 2021).

Considering instead the third strategy, Baldi *et al.* (2021) investigated the purification of leachate by pH variation. They found that this way was impractical due to the simultaneously precipitation of phosphorus with aluminium and iron at low values of pH (2–3.7). Similar results were found by Fang *et al.* (2018). At pH=3 almost the totality of iron precipitated, while the same happened for aluminium at pH=4. In addition, they studied the influence of precipitating agents on metals extraction and observed a slightly delay in precipitation of iron and aluminium in comparison to phosphorus by using $Ca(OH)_2$ instead of NaOH. However, a low significative reduction in terms of iron and aluminium content in the recovered material was detected and a high amount of gypsum was found. As a result, further efforts should be addressed to the optimisation of the phosphorus precipitation to increase the quality of the recovered material (Baldi *et al.* 2021; Liu *et al.* 2021).

Taking into account all the discussed current challenges, the aims of the present research work are: (i) the characterization of sewage sludge ash obtained from pilot-scale grate furnace in the view of phosphorus recovery; (ii) the comparison of the physical and chemical composition of bottom and cyclone ashes to determine the suitability of each type of ash for the phosphorus extraction; (iii) the investigation of factors beyond wet chemical extraction conditions that affect the phosphorus dissolution (upstream treatment characteristics, particle size dimension, loss on ignition – LOI, pH); (iv) the optimization of precipitation process conditions (pH, aging time, type of precipitating agents).

2. METHODS

2.1. Samples collection

Pelletized and dried sewage sludge from municipal wastewater was incinerated at 850 °C in a pilot-scale grate furnace located near the city of Milan (San Giuliano Milanese), in Italy, and engineered by VOMM Impianti e Processi SpA (Rozzano, Lombardy, Italy). The pelleting was adopted to simplify and reduce the fly ash capture systems and thus to protect the tube bundles of the boiler and the heat exchanger from erosion and fouling. The flat grid technology allows the treatment of dried sludge (85–90% dry matter content), which is deposited on the flat surface of the moving grid, while the combustion air is blown under the grate with a centrifugal fan. The combustion chamber is constituted by an adiabatic oven capable of withstanding the high temperatures (1,000 °C). As a first step, a dehydration phase takes place, leading to the removal of residual moisture

content. Then, an intermediate pyrolysis phase occurs, followed by a complete oxidation (combustion). To prevent an excessive NOx production, a flue gas recirculation system is applied and a selective non-catalytic reduction system (SNCR) is adopted. Ninety percent of ash accumulates at the end of the grid (bottom ash), thus favouring collection, while fly ash is subsequently captured and treated. Indeed, flue gas cleaning system consists of cyclones, bag filters, scrubber-type washing towers and activated carbons to fully meet the limits of emissions reported in the EU 2010/75 legislation. For this work, three experimental campaigns were conducted from August 2020 to April 2021. Each campaign lasted about 10 days, in which the furnace was operated continuously treating about 150 kg per hour. For each campaign, ashes were sampled three times a day during the sampling days (which were fixed at the beginning, at the middle and at the end of the operation). All samples were collected in PE plastic bottles and kept at room temperature. The total amount collected was about 2 kg of bottom ash (BA) and 2 kg of cyclone ash (CYC). Mean samples of BA collected during the operation period were named BA,1°, BA,2° and BA,3°, where the number denotes the experimental campaign (1°, 2° and 3°). In a similar way, CYC samples were named CYC,1°, CYC,2° and CYC,3° for the three campaigns. Three sub-samples of BA were collected during the third experimental campaign at the beginning, in the middle and at the end (named BA1,3°, BA2,3° and BA3,3°, respectively), to assess the influence of changes in the operating conditions of the mono-incineration plant. Sampling points are schematically shown in Figure S1.

2.2. Characterization of sewage sludge ash

BA samples were pounded by a manual mortar before characterization, while CYC samples were analysed as received. The ash humidity was measured by drying the samples in an oven at 105 °C overnight, while the LOI was evaluated by heating the dried samples in a laboratory standard muffle (LT 9/12 SKM Nabertherm, Germany) at 900 °C for 2 h. Particle size distribution was determined using a W. S. Tyler RO-TAP® Sieve shaker (Model RX-29) on a total ash mass of 200 g. Larger sieves used (850, 600, 425, 212 and 180 μm) met the Standard Test Sieve method (ASTM International 2020), while smaller sieves (0.125, 0.063 and 0.025 mm) were compliant with the ISO 3310–1:2016 method (ISO 2016). Ash pH was determined after 2 h leaching test using deionized water at a L/S (liquid-to-solid) ratio of 10:1, following the guideline of EN 12457-2 method (European Committee for Standardization 2002) and the optimized procedure described by Bontempi *et al.* (2010).

Ash total phosphorus content was evaluated using Hach Lange LCK 348 analytical kits, after acid mineralization with concentrated HNO_3 (65% w/w) at a sample-to-HNO_3 volume ratio of 5:2, according to EN 15956 (European Committee for Standardization 2011). The presence of most abundant elements (Al, Ca, Fe, K, Mg, Na) and metals/metalloids (As, Cd, Co, Cr, Cu, Hg, Ni, Pb, Sb, Tl, V, Zn) was determined by aqua regia mineralization followed by ICP-MS (Agilent, 7700 Series) analysis, according to UNI EN ISO 17294-1 (2007).

The crystalline composition of ash samples (BA and CYC) was investigated by X-ray diffraction (XRD) using a PANalytical X'Pert PRO diffractometer (Malvern Panalytical), at a voltage of 40 kV and a current of 40 mA, equipped with a Cu Kα anode. Phase identification was processed with Philips X'Pert software, associated with the crystallography open database (COD).

Morphological characterization of ash samples was performed by means of scanning electron microscopy combined with energy-dispersive X-ray spectrometry (SEM-EDXS) using a microscope LEO EVO 40 (Carl Zeiss), coupled with a probe for elemental and semiquantitative chemical analysis (Oxford Instruments). Secondary electron mode was used to investigate the sample morphology.

2.3. Phosphorus wet chemical extraction

Acid leaching was performed with 0.2 M H_2SO_4 prepared by dilution of high purity reagent (96% w/w) with ultra-pure water. BA sample collected in the first experimental campaign was used as received (raw), milled (with ball mill), pounded (with manual mortar) or split into four classes (class I, <0.063 mm; class II, 0.063–0.125 mm; class III, 0.180–0.212 mm; class IV, 0.425–0.600 mm). Mean BA samples collected in the second and third campaigns were directly pounded by manual mortar, while particle size lower than 0.212 mm was considered for the three sub-samples of BA from the third experimental campaign. CYC samples were always used as received.

For each experiment, 20 ± 0.1 g of dried ash were treated with 400 mL of 0.2 M H_2SO_4 solution. Agitation was provided by a magnetic stirrer (Variomag Poly 15) at a rotation speed of 650 rpm. Beakers were covered with watch glasses to prevent water evaporation. The suspension was then centrifuged at 3,500 rpm for 10 min and immediately filtered at 0.45-μm Whatman filter paper. Tests were performed at least in duplicate. PEE and extraction rates of metals/metalloids were calculated as reported by Boniardi *et al.* (2021).

While PEE was determined on all samples collected, only BA samples were used for the investigation of the influence of ash characteristics on phosphorus extraction. This choice was taken because about the 90% of total ash produced is constituted by bottom ash. In detail, BA,1° and BA,3° samples were selected to investigate the influence of particle size dimension and LOI.

2.4. Phosphorus precipitation

Precipitation tests were carried out using 30 mL of leachate obtained by the acid leaching of pounded BA (second experimental campaign). Only BA,2° sample was used to assess the influence of factors affecting the precipitation process. Preliminary precipitation tests were performed in triplicate to evaluate the amount of precipitated material and target pH at phosphorus thermodynamic equilibrium, as well as required aging time. Precipitation tests were conducted afterwards in duplicate under the following operating conditions: room temperature, 1 h as reaction time, 2 h as aging time. Different values of pH were studied: 2.5, 3.5, 5 and 8. To assess the influence of the precipitating agent on precipitated material characteristics, various procedures were compared. In the first trial, 0.1 M NaOH was gradually dosed until pH 3.5 followed by the addition of 0.5% $Ca(OH)_2$ until the target pH was reached. Such procedure was defined to prevent excessive co-precipitation of gypsum ($CaSO_4$) in the early stage of pH increase. In the second trial, only 0.1 M KOH was dosed. Obtained suspensions were filtered through a 0.45-μm Whatman filter paper and the phosphate content in filtered precipitate solution was determined. Overall, phosphorus precipitation efficiency (PPE) was calculated according to the procedure by Boniardi *et al.* (2021). In addition, the content of Al, Ca, Fe, Cu and Zn in the filtered solution was quantitatively determined by ICP-MS. Crystallinity of the precipitates was investigated using XRD. The same equipment previously described was used.

3. RESULTS AND DISCUSSION

3.1. Characterization of sewage sludge ash: grading curves, LOI, humidity, pH, crystalline forms and morphology

Grading curves of the investigated samples are depicted in Figure S2. As expected, CYC had a median particle size of 0.05 mm, while pounded BA samples were coarser with a median particle size of 0.1–0.2 mm. Raw pelletized BA instead had 90% of particles above 2 mm due to the type of configuration adopted for the sludge incineration. Similarly, Lin *et al.* (2018) investigated the particle size distribution of fly ash obtained from a hearth type incinerator and found a mean particle size of 0.07 mm, while bottom ash had a mean diameter of 0.8 mm. Li *et al.* (2017) instead dealt with sewage sludge ashes from fluidized bed incinerator and found a mean particle size of 0.056 mm, while Lee & Kim (2017) reported a mean particle size of 0.153 mm for fly ash collected from the bag filters. Donatello (2009) investigated the mean particle diameters of ashes collected from different UK incinerators and found a range of 0.008–0.263 mm, highlighting the influence of the type of incineration technology on particle size distribution. The large variability of size dimension was also reported by Ma & Rosen (2021) with a range of 0.05–1.5 mm. Thus, experimental results obtained in this study meet the mean size range reported in literature.

Considering the measure of unburned carbon content, CYC had LOI values below 1.6% for all campaigns, thus complying with the Directive 2010/75/EU (maximum value set at 5%). Instead, LOI values for BA,1°, BA,2°, and BA2,3° were above 5%, reaching a maximum value of 20.3% for BA,2°. This can be attributed to sub-optimal incineration conditions, which were optimized during the third experimental campaign by controlling flow rates of fed sludge, air, and residence time. As a result, LOI values for BA1,3° and BA3,3° were equal to 2.4% and 1.1%, respectively, while BA2,3° had still a higher LOI equal to 5.7%. Similarly, Zabielska-Adamska (2019) reported a LOI value of 4.72% for bottom ash obtained from a grate furnace. Krüger *et al.* (2014) provided different LOI values for ashes depending on combustion technique: 30 samples obtained from grate furnace showed a mean LOI of 4.8% with a maximum value of 13.1%. In addition, Cyr *et al.* (2007) reported an LOI value of 5.5% for ash obtained by fluidized bed incineration and indicated a mean literature value of 6.1% by analysing more than 20 sources. LOI values are affected by the combustion conditions and the type of incineration technology, so that low values can be achieved for good combustion.

As for pH, values in the range of 6.8–8.1 were measured for BA and 6.7–8.8 for CYC. Similarly, Li *et al.* (2017) reported a mean pH of 8.45 for ashes obtained from a fluidized bed incinerator. Humidity content was in the range of 0.1–0.8%, with a peak of 3.6% for BA,2°, probably due to storage conditions. Experimental data for LOI, pH and humidity are summarized in Table S2.

Experimental results of XRD analysis in Figure S3 revealed a similar crystalline composition for all BA samples: quartz [SiO_2] was detected as main phase, followed by a calcium iron phosphate phase, namely calcium hydrogen iron phosphate

$[Ca_9FeH(PO_4)_7]$ in BA,1° and BA,3°, and whitlockite $[Ca_8FeOH(PO_4)_6 \cdot 10H_2O]$ in BA,2°. Iron oxide $[Fe_2O_3]$ was identified in BA,1° and BA,3°, while potassium hydrogen phosphate $[KH_2PO_4]$ was present only in BA,2°. Moreover, anorthite $[CaAl_2Si_2O_8]$ was detected in BA,1°. The same analysis performed on CYC samples (Figure S4) showed again quartz as the main crystalline phase in all samples, with a little part of tridymite (another polymorphic form of $[SiO_2]$) in CYC,3°. $Ca_9FeH(PO_4)_7$ was identified in CYC,1° while $Ca_8FeOH(PO_4)_6 \cdot 10H_2O$ in CYC,2° and CYC,3°. Fe_2O_3 was detected in CYC,1° and CYC,3°, and another phosphate phase was found in CYC,1° and CYC,2°: sodium hydrogen phosphate $[Na_5H_{2.5}PO_5]$. In addition, small peaks revealed the presence of anhydrite $[CaSO_4]$ in CYC,3°. Similar results were reported by Gorazda *et al.* (2017): phosphorus in sewage sludge ash was present as calcium phosphate, iron as hematite, and aluminium as anorthite. Quartz and tridymite were also identified. In line with literature and presented experimental results, Abis *et al.* (2018) indicated quartz, hematite and whitlockite as the main crystallised minerals.

Morphologically, the CYC samples are very interesting. SEM images for CYC,1° and CYC,2° at different magnifications are shown in Figures 1 and 2, with the corresponding EDXS results reported in Table S3. The presence of spheres, mainly composed of Al, Si, P, Ca, Fe (areas 2-3-5 in CYC,1°-A and point 7 in CYC,1°-B), can be observed, as already reported by Fiameni *et al.* (2021). Area 1 in CYC,1°-A reveals an agglomerate mainly consisting of P and Fe, while area 4 in CYC,1°-A is a particular agglomerate composed of Mg and Si. Point 6 in CYC,1°-B is a Si-Al agglomerate, such as point 8, with a major presence of K. In CYC,2°-A, area 1 shows the absence of P, and a high percentage of Al and Si, while the chemical composition of the area 2 is similar to that of the spheres cited above, even if the surface is not smooth. Indeed, the image of CYC,2°-B shows that spheres have a rough surface and are internally hollow.

3.2. Characterization of sewage sludge ash: elemental composition

Tables 1 and 2 show the elemental composition of BA and CYC samples. Major elements, excluding heavy metals, were distributed as follows: *P*>Ca>Al>Fe>Mg>K>Na for BA samples, and Ca>*P*>Al>Fe>Mg>K>Na for CYC samples.

Mean concentrations of elements in pelletized and dried sewage sludge were compared to ash to calculate the enrichment factor, being reported in Figure S5. Most elements had an enrichment factor between 1 and 5 in BA and CYC samples, due to mass reduction during combustion. As, Cd, Pb, Sb and Zn showed an enrichment factor higher than 10 in CYC samples. Due to the higher volatility of those metals, they tend to concentrate in fine size ash, which is collected after flue gas treatments. Similar results were obtained by Cheng *et al.* (2020), that reported experimental data from multi-cyclone dust ash. On the contrary, observed enrichment factor for Fe (0.6–1.1) was much lower than expected. Indeed Cheng *et al.* (2020) observed an enrichment factor of 5–6 for all non-volatile elements including Fe. However, since the data refer to a fluidized bed incinerator, the enrichment factor for grate furnace can be different. To give a better insight of the enrichment factor for Fe, further investigation is needed.

Phosphorus content in sewage sludge ash samples ranged between 7.2% and 10.4%, thus perfectly aligned with literature data (4.9–11.9%) reported by Krüger & Adam (2015) for municipal sludge derived ash samples. In their study, they investigated ash chemical composition obtained by 24 incineration facilities equipped with different combustion technology (e.g.,

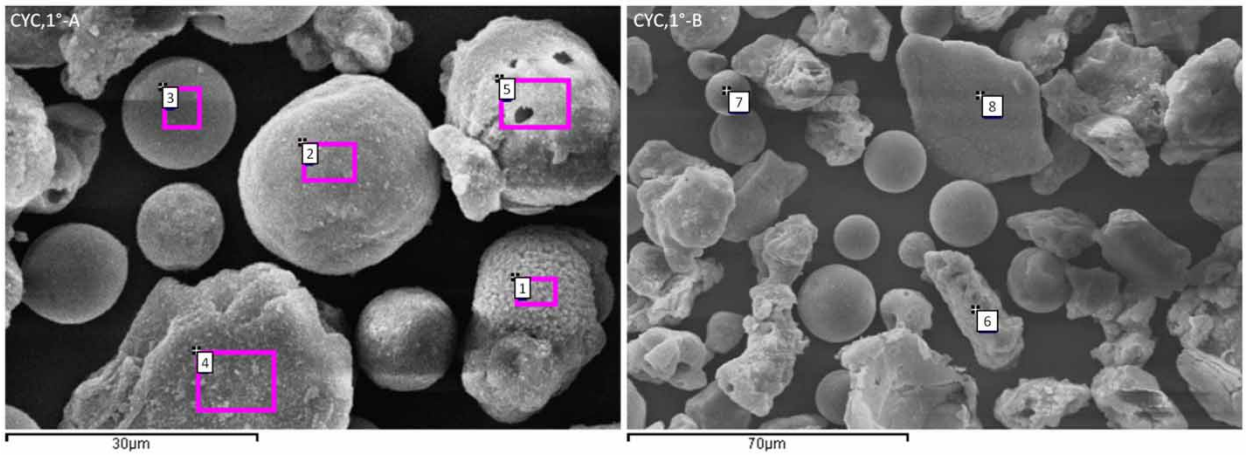

Figure 1 | SEM images (two magnification values: -A and -B) of cyclone ash obtained from the first experimental campaign (CYC,1°).

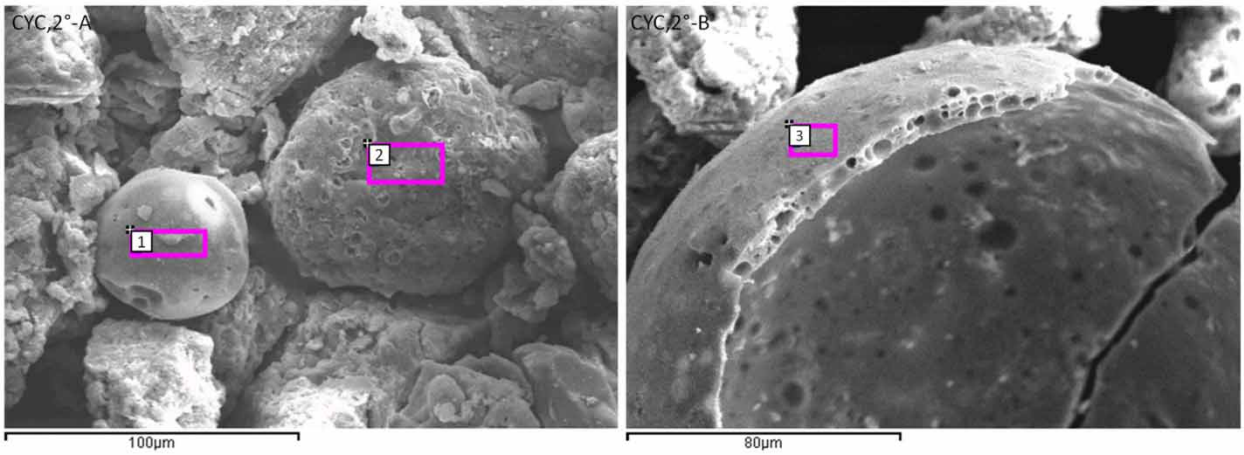

Figure 2 | SEM images (two magnification values: -A and -B) of cyclone ash obtained from the second experimental campaign (CYC,2°).

Table 1 | Element concentration (% or mg/kg) in bottom ash (BA) and cyclone ash (CYC) samples from the first and second experimental campaigns

	U.M.	BA,1°	CYC,1°	BA,2°	CYC,2°	Limit
P	%	7.2 ± 1.0	7.5 ± 1.1	7.2 ± 1.0	8.5 ± 1.2	–
Fe	%	3.4 ± 0.5	3.5 ± 0.5	2.2 ± 0.3	2.0 ± 0.3	–
Al	%	6.1 ± 0.9	6.7 ± 1.0	5.8 ± 0.8	6.1 ± 0.9	–
Ca	%	8.5 ± 1.2	8.9 ± 1.3	8.9 ± 1.3	9.1 ± 1.3	–
K	%	0.7 ± 0.1	0.8 ± 0.1	0.5 ± 0.1	0.6 ± 0.1	–
Mg	%	1.4 ± 0.2	1.2 ± 0.2	0.9 ± 0.1	1.0 ± 0.1	–
Na	%	0.32 ± 0.05	0.3 ± 0.04	0.2 ± 0.02	0.2 ± 0.03	–
As	mg kg^{-1}	32.9 ± 4.7	**92.2 ± 13.0**	25.8 ± 3.7	**49.7 ± 7.0**	40
Cd	mg kg^{-1}	0.31 ± 0.04	**76.8 ± 10.9**	0.51 ± 0.07	**37.1 ± 5.2**	1.5
Co	mg kg^{-1}	31.8 ± 4.5	26.3 ± 3.7	16.6 ± 2.4	20.9 ± 3	–
Cr	mg kg^{-1}	**441.6 ± 62.5**	**468.8 ± 66.3**	**426.4 ± 60.3**	**640.2 ± 90.5**	2
Cu	mg kg^{-1}	**1,014.6 ± 143.5**	**1,274.0 ± 180.2**	**1,179.4 ± 166.8**	**1,202.6 ± 170.1**	600
Hg	mg kg^{-1}	0.49 ± 0.07	0.64 ± 0.09	0.54 ± 0.08	0.54 ± 0.07	1
Ni	mg kg^{-1}	**552.0 ± 78.1**	**560.4 ± 72.3**	**605.5 ± 85.6**	**514.1 ± 72.7**	100
Pb	mg kg^{-1}	**124.5 ± 17.6**	**2,522.8 ± 356.8**	**213.9 ± 30.3**	**802.5 ± 113.5**	120
Sb	mg kg^{-1}	6.6 ± 0.9	6.1 ± 0.8	7.6 ± 1.1	6.7 ± 0.9	–
Tl	mg kg^{-1}	0.19 ± 0.03	0.36 ± 0.05	0.20 ± 0.03	0.35 ± 0.05	–
V	mg kg^{-1}	66.3 ± 9.4	72.7 ± 10.3	49.9 ± 7.1	52 ± 7.4	–
Zn	mg kg^{-1}	**2,381.6 ± 336.8**	**6,244.8 ± 883.2**	**3,229.7 ± 456.8**	**3,197.2 ± 452.2**	1,500

Reported limits refer to European regulation for fertilizer application (EU 2019/1009). Limit for chromium (Cr) refers to Cr (VI), while the content in the investigated ashes refer to total chromium. Values in bold indicate the exceedance of the limits

fluidized bed, grate furnace, multiple hearth firing). The highest phosphorus concentrations were observed in the third experimental campaign (April), reaching a maximum concentration of about 9% in BA and 10.4% in CYC. The lowest phosphorus concentrations (7.2% for BA and 7.5% for CYC) were measured in the second experimental campaign (August). The same trend was reported by Krüger *et al.* (2014), who analysed the monthly variations of the phosphorus content in ashes for different facilities. They reported peaks of phosphorus concentration in February, March and April, and a decline of phosphorus content from June to August. Variation in phosphorus concentration can be explained by the common fluctuations of inlet

Table 2 | Element concentration (% or mg/kg) in bottom ash (BA) and cyclone ash (CYC) samples from the third experimental campaigns

	U.M.	BA1,3°	BA2,3°	BA3,3°	CYC,3°	Limit
P	%	9.9 ± 1.4	9.0 ± 1.3	8.0 ± 1.1	10.4 ± 1.5	–
Fe	%	1.9 ± 0.3	2.0 ± 0.3	2.1 ± 0.3	1.7 ± 0.2	–
Al	%	9.0 ± 1.3	7.4 ± 1.0	8.6 ± 1.2	9.4 ± 1.3	–
Ca	%	8.5 ± 1.2	5.8 ± 0.8	8.2 ± 1.2	8.8 ± 1.2	–
K	%	0.48 ± 0.06	0.57 ± 0.08	0.49 ± 0.07	0.54 ± 0.08	–
Mg	%	1.3 ± 0.2	1.2 ± 0.2	1.3 ± 0.2	1.3 ± 0.2	–
Na	%	0.34 ± 0.05	0.33 ± 0.05	0.39 ± 0.06	0.29 ± 0.04	–
As	mg kg^{-1}	26.6 ± 3.8	**60.2 ± 8.5**	27.8 ± 3.9	**227.6 ± 32.2**	40
Cd	mg kg^{-1}	0.19 ± 0.03	0.19 ± 0.03	0.20 ± 0.03	**139.1 ± 19.7**	1.5
Co	mg kg^{-1}	13.3 ± 1.9	12.3 ± 1.7	12.7 ± 1.8	12.1 ± 1.7	–
Cr	mg kg^{-1}	**226.4 ± 32.0**	**218.5 ± 31.0**	**209.7 ± 29.7**	**423.3 ± 59.9**	2
Cu	mg kg^{-1}	**1,174.8 ± 166.1**	**1,244.6 ± 176.0**	**1,418.7 ± 200.6**	**1,184.8 ± 167.6**	600
Hg	mg kg^{-1}	0.58 ± 0.08	0.56 ± 0.08	0.52 ± 0.07	0.57 ± 0.08	1
Ni	mg kg^{-1}	**606 ± 85.7**	**197.5 ± 27.9**	**604.4 ± 85.5**	**586.2 ± 82.9**	100
Pb	mg kg^{-1}	104.3 ± 14.8	83.4 ± 11.8	66.1 ± 9.4	**6,317.7 ± 893.5**	120
Sb	mg kg^{-1}	7.4 ± 1.0	7.2 ± 1.0	6.9 ± 1.0	9.3 ± 1.3	–
Tl	mg kg^{-1}	0.20 ± 0.03	0.20 ± 0.03	0.20 ± 0.03	0.56 ± 0.08	–
V	mg kg^{-1}	49.5 ± 7.0	57.6 ± 8.1	52.2 ± 7.4	45.5 ± 6.4	–
Zn	mg kg^{-1}	**1,810 ± 256.0**	**1,604 ± 226.8**	1,479.3 ± 209.2	**14,792.4 ± 2,092.0**	1,500

Limits refer to European regulation for fertilizer application fertilizer application (EU 2019/1009). Values in bold indicate the exceedance of the limits.

phosphorus concentration during the year and different phosphorus removal performances of the wastewater treatment plant (WWTP). Moreover, Krüger *et al.* (2014) suggested that the variation of food habits, leisure time and higher temperature in summer may be responsible for the drop of phosphorus concentration. It is reasonable to imagine that during summer people have more leisure time and those who are living in metropolitan cities such as Milan can travel to touristic locations. This can reduce the influent phosphorus loading rate at the WWTP, affecting the phosphorus content in the sludge and in the derived ash (Krüger *et al.* 2014). In addition, seasonal changes in P removal efficiency at WWTP can be related to phosphorus accumulating organisms (PAOs) performances fluctuations. Thus, temperature can change the dynamics of the microbial communities, raising possible competition of phosphorus accumulating organisms (PAOs) with other bacteria (Erdal *et al.* 2003; Ni *et al.* 2021).

Considering the two types of sewage sludge ashes collected within the same experimental campaign, CYC samples had a slightly higher phosphorus content compared to BA samples. Despite the non-volatility of phosphorus, it tended to concentrate in the finer fraction. This could be explained by the presence of reducing combustion conditions in the upper layer of the fuel bed, promoting the vaporisation of phosphorus (Han *et al.* 2009). As highlighted by Razmjoo *et al.* (2016), the complete consumption of oxygen takes place in the combustion layer of the fuel bed, resulting in reducing conditions in the fuel layers above. Instead, Gorazda *et al.* (2017) found a phosphorus concentration in BA (9.9%) slightly higher than CYC (9.7%).

As for the content of Fe and Al in ashes, higher concentrations of Al were observed in all experimental campaigns due to the use of Al salts in the WWTP. Within the experimental campaigns, higher concentration of Fe, Al and Ca were observed in CYC samples in comparison to BA samples. An exception was observed for Fe content in the second and third experimental campaigns. Similar results were reported by Gorazda *et al.* (2017): Fe content at 6.0% and 6.7%, Al content at 4.6% and 7.3%, and Ca content at 11.2% and 12% in BA and CYC were measured, respectively. High concentrations of Fe and Al in ashes are critical as they limit the quality of the recovered material, due to their precipitation with phosphorus.

Concerning the content of metals and metalloids in BA and CYC samples, Zn was the most abundant metal (1,479–14,792 mg/kg) followed by Cu (1,014–1,418 mg/kg). It clearly emerged from Table 2 that the Zn content of 14,792 ± 2,092 mg/kg (CYC,3°) is out of the range (644–2,535 mg/kg) reported in literature (Ottosen *et al.* 2013; Krüger

et al. 2014; Herzel *et al.* 2016; Wang *et al.* 2018; Benassi *et al.* 2019; Liang *et al.* 2019). Such outlier can be explained by an exceptional industrial load at the WWTP, as confirmed by the WWTP manager. Table S4 summarizes the heavy metal concentrations in sewage sludge ashes reported in literature.

In general, regarding the distribution of metals and metalloids in samples, it was highlighted that semi-volatile elements such as Zn, Pb, Cd and As tended to concentrate in the finer particles (CYC), while the non-volatile elements (Cr, Cu, Ni and V) equally distributed among the two types of ashes (Toledo *et al.* 2005; Van de Velden *et al.* 2008; Nzihou & Stanmore 2013). Shao *et al.* (2008) found similar results, indicating that Pb and Zn were mostly present in fly ash, while other heavy metals such as Cr, Ni, V resulted equally distributed between bottom and fly ash. Same observations were reported by Cheng *et al.* (2020), pointing out that higher enrichments of Pb and Cd were found for cyclone ash because of temperature and particle size.

As a result, BA samples, corresponding to the 90% of total ash produced during combustion, showed a lower level of metals contamination if compared to CYC samples, whose hazardousness is mainly due to high concentrations of As, Cd, Cr, Pb and Zn. Overall, both ash typologies do not comply with the limits for fertilizer applications (EU 2019/1009), resulting in a ban for agricultural use.

3.3. Factors affecting the phosphorus extraction efficiency

Experimental results demonstrated that not only the operating conditions of the chemical wet extraction can affect the PEE, but also the chemical-physical characteristics of sewage sludge ash, as particle size dimension, LOI and pH.

The influence of particles size dimension was studied considering the sample BA,1°. As expected, BA in the form of pellets (90% of particles above 2 mm) had the lowest PEE (56%), while BA milled (with ball mill) and pounded (with manual mortar) showed higher PEE (80% and 78%, respectively). Small particle size ensures a larger contact area between solid particles and extractant. Thus, the extractant can probably travel into pores and reach the reaction zone in a shorter time. Additional tests were performed considering four different particle size classes of pounded BA,1° (class I, <0.063 mm; class II, 0.063–0.125 mm; class III, 0.180–0.212 mm; class IV, 0.425–0.600 mm). Experimental results are reported in Figure S6. Particle size dimension lower than 0.212 mm ensured a good PEE (>70%), while higher particle size dimension (0.425–0.600 mm) resulted in lower PEE. In conclusion, very fine particle size (lower than 0.063 mm) is not strictly required. Instead, too small particles can be tightly packed, decreasing the mechanisms of diffusion and mass transport.

Furthermore, the influence of LOI on PEE was investigated considering the three BA sub-samples collected in the third experimental campaign, in which combustion conditions (mass flow rate and residence time) were slightly changed for process optimization. To avoid the influence of particle size dimension, sewage sludge ashes with particle size lower than 0.212 mm were considered, while acid extraction conditions were kept constant. As a result, the highest PEE (85.6%) was reached by BA3,3° sample, which had the lowest LOI (1.1%). Thus, unburned fractions may subtract extracting capacity to the acid solution, causing a decrease of the process selectivity towards phosphorus. In addition, formation of different species containing the unburned fraction can affect the solubility of phosphate-bearing compounds. These experimental results evidence the importance of optimizing the combustion conditions in the design of a process aimed at phosphorus recovery.

Experimental results from leaching tests in deionized water revealed that the pH of BA samples was between 6.8 and 8.1, while it was between 6.7 and 8.8 for CYC samples. In general, sewage sludge ash samples with pH around 7 (BA,3°, BA2,3° and CYC,1°) showed the highest PEE. Instead, basic pH slightly lowers the extraction efficiency possibility due to ash basicity that tends to neutralize the acidic pH.

The chemical composition of sewage sludge ash, which is related to the incineration technology, can also affect the PEE. Liu *et al.* (2021) highlighted indeed the importance of upstream treatment conditions in the phosphorus speciation in sewage sludge ash. Figure 3 shows the experimental results of leaching tests conducted on the investigated samples.

Overall, mean phosphorus concentration in leachate varied between 2,823 and 3,775 mg/L, while PEE ranged between 71% and 86%. The first and second experimental campaigns had comparable phosphorus concentrations in leachate for both ashes (2,823 and 3,325 mg/L), while the third campaign showed higher phosphorus concentration in leachate (from 3,425 to 3,775 mg/L). The highest concentrations were measured in the samples that had the highest phosphorus content in the ash (BA1,3° and CYC,3°), while the highest PEE was reached by BA3,3° (85.6%) and CYC,1° (83.0%) samples. Instead, lowest PEE was reached by BA,2° (75.0%) and CYC,3° (69.1%) samples. Thus, a high phosphorus concentration in the leachate (e.g., observed in CYC,3°) does not necessarily correspond to a high PEE, since the extraction efficiency is calculated as the ratio between the mass of phosphorus in the leachate and the mass of phosphorus in the ash.

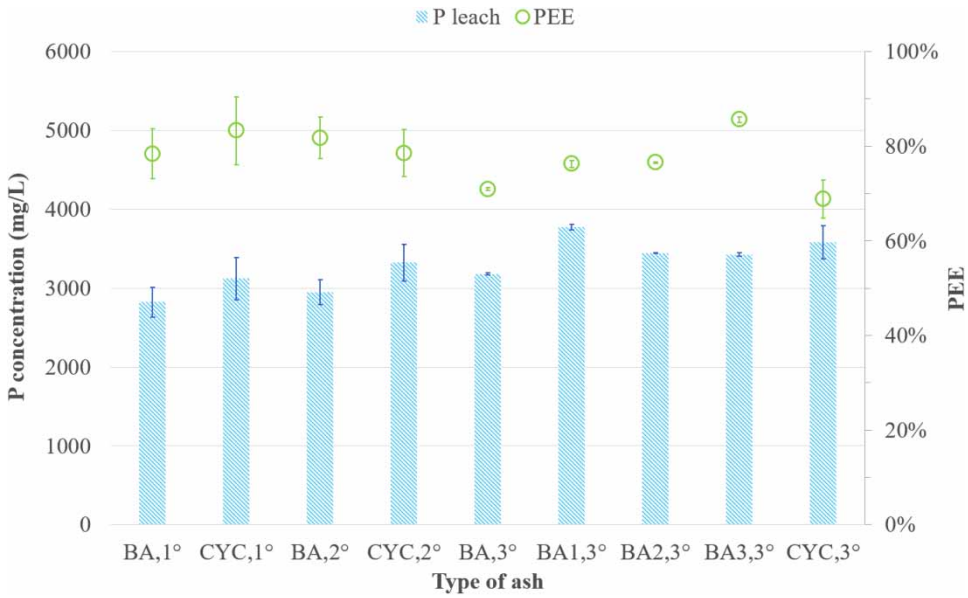

Figure 3 | Phosphorus concentration in leachate (as mg/L) and PEE for the investigated samples.

The decrease of PEE for CYC samples can be attributed to the higher content of Al in CYC,3° sample (9.4%) if compared to CYC,1°–2° sample (6.0–6.7%). Kalmykova & Karlfeldt Fedje (2013) pointed out that a high content of Al in sewage sludge ash can significantly decrease the PEE, while Gorazda *et al.* (2017) reported that high concentration of Al may cause precipitation of phosphate compounds during extraction. Therefore, phosphate compounds can be present in larger extent in the acidic solid residue, decreasing the phosphorus concentration in leachate. On the contrary, when Fe is immobilised in the hematite phase, which is slightly insoluble in strong acid, the extraction becomes more selective towards phosphorus compounds (Gorazda *et al.* 2017). Indeed, Ma & Rosen (2021) recommended the acid extraction only for Fe-rich sewage sludge ashes. However, even if the iron co-dissolution could be limited, the level of Fe content in the ash is the main parameter affecting the Fe concentration in the leachate and in the precipitated product. Thus, the use alone of biological P removal at the WWTP would be the best solution for decreasing the Al and Fe content in the sludge and thus in the ash.

3.4. Co-dissolution of undesired elements

Because of strong acidic conditions achieved during leaching tests (pH between 1.3 and 2), undesired elements such as metals and metalloids can dissolve. Figure S7 shows the percentage of elements passing in solution, while Table S5 summarises their concentrations in liquid phase. In general, Cr, Ni and Pb tended to concentrate in the acidic solid residues, while 58–91% of As and 54–100% of Cd easily passed in solution. Kim & Kazonich (2004) highlighted that the non-silicate phase present in sewage sludge ashes can be responsible for this higher solubility. In addition, Fang *et al.* (2018) reported a nearly completely dissolution of As, and Li *et al.* (2017) obtained an extraction rate of 75%. Considering the most abundant metals (Fe and Al), the extraction rates observed were between 26–74% for Fe and 30–100% for Al. The lowest extraction rate of Al was observed for BA,3° and CYC,3° samples, which had also a low PEE. Regarding the most present metals (Zn and Cu), extraction rates between 25% and 81% were observed. Overall, leachates derived from CYC samples showed higher contamination in comparison to leachates from BA samples. Thus, BA samples can be preferred for phosphorus extraction and subsequent recovery due to the lower contamination.

3.5. Phosphorus precipitation

Some flocculation phenomena started at nearly pH 2, increasing its intensity with the addition of basic compounds. At pH 3, about 80–90% of the total mass of precipitated material was formed, while the remaining part (20–10%) precipitated within pH 7. Experimental results of preliminary tests, shown in Figure S8 and Figure S9, revealed that aging time of 2 h and pH of 3.5 were sufficient to reach the phosphorus thermodynamic equilibrium, to have a high PPE and phosphorus content.

Precipitation tests conducted afterwards revealed that the type of precipitating agent (NaOH, $Ca(OH)_2$, KOH) did not strongly affect the amount of precipitated phosphorus. Thus, more than 90% of phosphorus precipitates from leachate within pH 3.5. This is in accordance with Fang *et al.* (2018), who reported the occurrence of phosphorus precipitation within pH 3.2–3.9.

The precipitated material showed high phosphorus content (16–21%) in the first stage of pH increase (Figure 4), followed by a low decline due the co-precipitation of undesirable elements. Thus, the increase of the mass of the recovered material implied a higher phosphorus dilution. As a result, pH 3.5 and 5 can be considered to be the most suitable values for ensuring both a high PPE (>90%) and phosphorus content (17%).

For all samples, XRD analysis revealed the absence of crystalline forms. As a result, most of the phosphorus in the recovered material is present in amorphous phases, thus possibly easily available for the plant root. It could be interesting to further study the crystallization kinetics of the precipitates, to investigate the formation of crystalline Ca, Al, or Fe phosphates.

Considering the co-precipitation of other elements, as highlighted by Ito *et al.* (2013), aluminium and iron phosphates combined with their hydroxides are the major compounds formed between pH 3 and 4, while calcium phosphates prevail from pH 4. Similarly, Baldi *et al.* (2021) assumed the forms of phosphorus precipitated as $Ca_3(PO4)_2$, $FePO_4$ and $AlPO_4$ at pH 3.7. In addition, Fang *et al.* (2018) reported that the Fe precipitated at pH lower than 2.6 may correspond to goethite or hematite. The analysis of the filtrate solution obtained after precipitation tests confirmed the complete precipitation of Al and Fe at pH 5. Instead, the complete precipitation of Zn and Cu occurred at pH 8. Figure S10 shows the precipitation efficiency of investigated elements (P, Al, Fe, Ca, Zn and Cu) for the different precipitation tests. It can be noted that the type of precipitating agent (NaOH followed by $Ca(OH)_2$ and KOH) did not strongly affect the precipitation efficiencies. An unexpected behaviour was observed for Zn, since a small delay in its precipitation at pH 2.5 occurred, while dosing NaOH instead of KOH. Overall, at pH 3.5, 40% of Zn and 20% of Cu precipitated, while at pH 5 about 65% of Zn and 80% of Cu precipitated. At the same time, Ito *et al.* (2013) reported 40% of Zn precipitation and 50% Cu at pH 4, confirming the co-precipitation of those elements with phosphorus.

In conclusion, the quality of the recovered material decreased while increasing the precipitation pH. The presence of Al and Fe can reduce the plant availability of the recovered product, as reported by Liang *et al.* (2019). In addition, Liu *et al.* (2021) highlighted the need for process optimization for Ca-P product recovery, as innovative strategies for leachate decontamination are required. They suggested the use of new bio-based adsorbent to remove the interfering ions before precipitation.

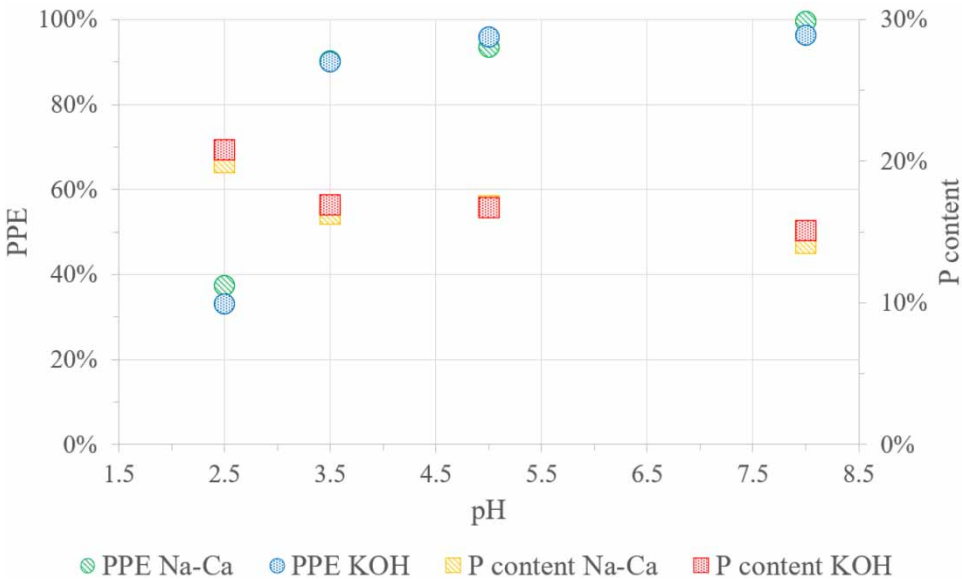

Figure 4 | Influence of the type of precipitating agent on PEE, phosphorus content and pH (sample BA,2° sample). Na-Ca refers to dosage of NaOH until pH 3.5 followed by dosage of $Ca(OH)_2$ for the higher pH ranges (from pH 3.5 to 5 and from pH 3.5 to 8).

4. CONCLUSIONS

- Grate furnace is a viable option for sewage sludge ash mono-incineration in the view of phosphorus recovery. Acid leaching of bottom ash (BA) and cyclone ash (CYC) showed a mean phosphorus extraction efficiency (PEE) between 69% and 86% at 0.2 M H_2SO_4, L/S of 20:1, 2 h as contact time and room temperature.
- BA samples showed a slightly lower phosphorus content (7.2–9.9%) and a much lower level of heavy metal contamination with respect to CYC samples. As a result, BA, representing the 90% of the ashes produced, is more suitable for the phosphorus extraction process.
- Upstream treatment characteristics such as the type of phosphorus-removal technology used at WWTP can affect the PEE and the quality of the recovered material. High concentration of Al in ash can be responsible for a decrease of the extraction capacity. The lowest PEE was indeed achieved by the sample with the highest Al content in the ash (9.4%). At the same time, Fe content in the ash of 3.5% can affect the quality of the recovered material, due to formation of iron phosphates compounds in the final product.
- Ash physical characteristics influence the PEE. Particle size dimension lower than 0.212 mm turned out to be sufficiently fine to provide a good contact surface between solid particles and the extractant. At the same time, a good combustion efficiency showed better extraction performances: the lower the LOI, the higher the PEE.
- Positioning the recovery of P as first design parameter is of paramount importance. Thus, the type of combustion technology can strongly influence the chemical composition and morphology of ashes.
- Key factor for ensuring a high phosphorus precipitation efficiency (PPE) and phosphorus content is pH, while precipitating agents do not have a strong influence. pH in the range of 3.5–5 ensures a PPE higher than 90%, a P content between 16–17% and a low co-dissolution of Cu and Zn.
- Further investigations and strategies on leachate decontamination (e.g., using bio-based adsorbents or performing ashes inertization prior to acid leaching) are needed for ensuring a high-quality fertilizer material. Thus, the minimization of heavy metals, Fe and Al content is required.

ACKNOWLEDGEMENTS

This work was partially funded by Region Lombardy (Italy) within the research project 'PerformWater_2030' (Decree DGR N. 5245/2016 – AZIONE I.1.B.1.3 – ASSE I POR FESR 2014–2020 – CUP E46D17000120009). The authors would like to thank VOMM Impianti e Processi for the assistance in ash sampling and for providing information about the incineration plant. The authors would also like to gratefully thank Rea Dalmine (Greenthesis Group, Dalmine, Italy) for funding the PhD grant of Gaia Boniardi.

DATA AVAILABILITY STATEMENT

All relevant data are included in the paper or its Supplementary Information.

REFERENCES

Abis, M., Calmano, W. & Kuchta, K. 2018 Innovative technologies for phosphorus recovery from sewage sludge ash. *Detritus* **1**, 23–29. https://doi.org/10.26403/detritus/2018.23.

ASTM International 2020 ASTM E-11: Standard Specification for Woven Wire Test Sieve Cloth and Test Sieves.

Baldi, M., Martinotti, A., Sorlini, S., Katsoyiannis, I., Abbà, A., Carnevale Miino, M. & Collivignarelli, M. 2021 Extraction and purification of phosphorus from the ashes of incinerated biological sewage sludge. *Water* **13**, 1102. https://doi.org/10.3390/w13081102.

Benassi, L., Zanoletti, A., Depero, L. E. & Bontempi, E. 2019 Sewage sludge ash recovery as valuable raw material for chemical stabilization of leachable heavy metals. *Journal of Environmental Management* **245**, 464–470. https://doi.org/10.1016/j.jenvman.2019.05.104.

Biswas, B. K., Inoue, K., Harada, H., Ohto, K. & Kawakita, H. 2009 Leaching of phosphorus from incinerated sewage sludge ash by means of acid extraction followed by adsorption on orange waste gel. *Journal of Environmental Sciences* **21**, 1753–1760. https://doi.org/10.1016/S1001-0742(08)62484-5.

Boniardi, G., Turolla, A., Fiameni, L., Gelmi, E., Malpei, F., Bontempi, E. & Canziani, R. 2021 Assessment of a simple and replicable procedure for selective phosphorus recovery from sewage sludge ashes by wet chemical extraction and precipitation. *Chemosphere* **285**, 131476. https://doi.org/10.1016/j.chemosphere.2021.131476.

Bontempi, E., Zacco, A., Borgese, L., Gianoncelli, A., Ardesi, R. & Depero, L. E. 2010 A new method for municipal solid waste incinerator (MSWI) fly ash inertization, based on colloidal silica. *Journal of Environmental Monitoring* **12**, 2093. https://doi.org/10.1039/c0em00168f.

Cheng, Y., Oleszek, S., Shiota, K., Oshita, K. & Takaoka, M. 2020 Comparison of sewage sludge mono-incinerators: mass balance and distribution of heavy metals in step grate and fluidized bed incinerators. *Waste Management* **105**, 575–585. https://doi.org/10.1016/j.wasman.2020.02.044.

Chrispim, M. C., Scholz, M. & Nolasco, M. A. 2019 Phosphorus recovery from municipal wastewater treatment: critical review of challenges and opportunities for developing countries. *Journal of Environmental Management* **248**, 109268. https://doi.org/10.1016/j.jenvman.2019.109268.

Cyr, M., Coutand, M. & Clastres, P. 2007 Technological and environmental behavior of sewage sludge ash (SSA) in cement-based materials. *Cement and Concrete Research* **37**, 1278–1289. https://doi.org/10.1016/j.cemconres.2007.04.003.

Desmidt, E., Ghyselbrecht, K., Zhang, Y., Pinoy, L., Van der Bruggen, B., Verstraete, W., Rabaey, K. & Meesschaert, B. 2015 Global phosphorus scarcity and full-scale P-recovery techniques: a review. *Critical Reviews in Environmental Science and Technology* **45**, 336–384. https://doi.org/10.1080/10643389.2013.866531.

Directive 2010/75/EU. Available from: http://data.europa.eu/eli/dir/2010/75/2011-01-06

Donatello, S. 2009 Characteristics of incinerated sewage sludge ashes: potential for phosphate extraction and re-use as a pozzolanic material in construction products. https://doi.org/10.13140/RG.2.2.33926.63040

Donatello, S. & Cheeseman, C. R. 2013 Recycling and recovery routes for incinerated sewage sludge ash (ISSA): a review. *Waste Management* **33**, 2328–2340. https://doi.org/10.1016/j.wasman.2013.05.024.

Erdal, U. G., Erdal, Z. K. & Randall, C. W. 2003 The competition between PAOs (phosphorus accumulating organisms) and GAOs (glycogen accumulating organisms) in EBPR (enhanced biological phosphorus removal) systems at different temperatures and the effects on system performance. *Water Science and Technology* **47**, 1–8. https://doi.org/10.2166/wst.2003.0579.

European Commission (EC) 2017. Available from: https://ec.europa.eu/growth/sectors/raw-materials/specific-interest/critical_en

European Committee for Standardization 2002 EN 12457–2 Characterisation of waste – leaching – compliance test for leaching of granular waste materials and sludges – Part 2: One stage batch test at a liquid to solid ratio of 10 L/kg for materials with particle size below 4 Mm (without or with size reduction).

European Committee for Standardization 2011 EN 15956 Fertilizers – extraction of phosphorus soluble in mineral acids.

Fahimi, A., Federici, S., Depero, L. E., Valentim, B., Vassura, I., Ceruti, F., Cutaia, L. & Bontempi, E. 2021 Evaluation of the sustainability of technologies to recover phosphorus from sewage sludge ash based on embodied energy and CO2 footprint. *Journal of Cleaner Production* **289**, 125762. https://doi.org/10.1016/j.jclepro.2020.125762.

Fang, L., Li, J., Donatello, S., Cheeseman, C. R., Wang, Q., Poon, C. S. & Tsang, D. C. W. 2018 Recovery of phosphorus from incinerated sewage sludge ash by combined two-step extraction and selective precipitation. *Chemical Engineering Journal* **348**, 74–83. https://doi.org/10.1016/j.cej.2018.04.201.

Fang, L., Wang, Q., Li, J., Poon, C. S., Cheeseman, C. R., Donatello, S. & Tsang, D. C. W. 2020 Feasibility of wet-extraction of phosphorus from incinerated sewage sludge ash (ISSA) for phosphate fertilizer production: a critical review. *Critical Reviews in Environmental Science and Technology* 1–33. https://doi.org/10.1080/10643389.2020.1740545.

Fiameni, L., Assi, A., Fahimi, A., Valentim, B., Moreira, K., Predeanu, G., Slăvescu, V., Vasile, B. Ş., Nicoară, A. I., Borgese, L., Boniardi, G., Turolla, A., Canziani, R. & Bontempi, E. 2021 Simultaneous amorphous silica and phosphorus recovery from rice husk poultry litter ash. *RSC Advances* **11**, 8927–8939. https://doi.org/10.1039/D0RA10120F.

Franz, M. 2008 Phosphate fertilizer from sewage sludge ash (SSA). *Waste Management* **28**, 1809–1818. https://doi.org/10.1016/j.wasman.2007.08.011.

Gorazda, K., Wzorek, Z. & Jodko, M. 2007 The influence of thermal processing of sewage sludge on the usage properties of the formed ash. *Polish Journal of Chemical Technology* **9**, 21–27. https://doi.org/10.2478/v10026-007-0083-y.

Gorazda, K., Tarko, B., Wzorek, Z., Kominko, H., Nowak, A. K., Kulczycka, J., Henclik, A. & Smol, M. 2017 Fertilisers production from ashes after sewage sludge combustion – a strategy towards sustainable development. *Environmental Research* **154**, 171–180. https://doi.org/10.1016/j.envres.2017.01.002.

Han, J., Kanchanapiya, P., Sakano, T., Mikuni, T., Furuuchi, M. & Wang, G. 2009 The behaviour of phosphorus and heavy metals in sewage sludge ashes. *IJEP* **37**, 357. https://doi.org/10.1504/IJEP.2009.026054.

Herzel, H., Krüger, O., Hermann, L. & Adam, C. 2016 Sewage sludge ash – a promising secondary phosphorus source for fertilizer production. *Science of The Total Environment* **542**, 1136–1143. https://doi.org/10.1016/j.scitotenv.2015.08.059.

Hong, K.-J., Tarutani, N., Shinya, Y. & Kajiuchi, T. 2005 Study on the recovery of phosphorus from waste-activated sludge incinerator ash. *Journal of Environmental Science and Health, Part A* **40**, 617–631. https://doi.org/10.1081/ESE-200046614.

International Organization for Standardization (ISO) 2016 Test Sieves – Technical Requirements and Testing Test Sieves of Metal Wire Cloth (ISO 3310-1:2016).

Ito, A., Yamada, K., Ishikawa, N. & Umita, T. 2013 Separation of metals and phosphorus from incinerated sewage sludge ash. *Water Science and Technology* **67**, 2488–2493. https://doi.org/10.2166/wst.2013.142.

Kalmykova, Y. & Karlfeldt Fedje, K. 2013 Phosphorus recovery from municipal solid waste incineration fly ash. *Waste Management* **33**, 1403–1410. https://doi.org/10.1016/j.wasman.2013.01.040.

Kim, A. G. & Kazonich, G. 2004 The silicate/non-silicate distribution of metals in fly ash and its effect on solubility. *Fuel* **83**, 2285–2292. https://doi.org/10.1016/j.fuel.2004.06.005.

Krüger, O. & Adam, C. 2015 Recovery potential of German sewage sludge ash. *Waste Management* **45**, 400–406. https://doi.org/10.1016/j.wasman.2015.01.025.

Krüger, O., Grabner, A. & Adam, C. 2014 Complete survey of German sewage sludge ash. *Environmental Science & Technology* **48**, 11811–11818. https://doi.org/10.1021/es502766x.

Lee, M. & Kim, D.-J. 2017 Identification of phosphorus forms in sewage sludge ash during acid pre-treatment for phosphorus recovery by chemical fractionation and spectroscopy. *Journal of Industrial and Engineering Chemistry* **51**, 64–70. https://doi.org/10.1016/j.jiec.2017.02.013.

Li, J., Xue, Q., Fang, L. & Poon, C. S. 2017 Characteristics and metal leachability of incinerated sewage sludge ash and air pollution control residues from Hong Kong evaluated by different methods. *Waste Management* **64**, 161–170. https://doi.org/10.1016/j.wasman.2017.03.033.

Li, B., Boiarkina, I., Yu, W., Huang, H. M., Munir, T., Wang, G. Q. & Young, B. R. 2019a Phosphorous recovery through struvite crystallization: challenges for future design. *Science of The Total Environment* **648**, 1244–1256. https://doi.org/10.1016/j.scitotenv.2018.07.166.

Li, B., Udugama, I. A., Mansouri, S. S., Yu, W., Baroutian, S., Gernaey, K. V. & Young, B. R. 2019b An exploration of barriers for commercializing phosphorus recovery technologies. *Journal of Cleaner Production* **229**, 1342–1354. https://doi.org/10.1016/j.jclepro.2019.05.042.

Liang, S., Chen, H., Zeng, X., Li, Z., Yu, W., Xiao, K., Hu, J., Hou, H., Liu, B., Tao, S. & Yang, J. 2019 A comparison between sulfuric acid and oxalic acid leaching with subsequent purification and precipitation for phosphorus recovery from sewage sludge incineration ash. *Water Research* **159**, 242–251. https://doi.org/10.1016/j.watres.2019.05.022.

Lin, W. Y., Ng, W. C., Wong, B. S. E., Teo, S. L.-M., Sivananthan, G. d., Baeg, G. H., Ok, Y. S. & Wang, C.-H. 2018 Evaluation of sewage sludge incineration ash as a potential land reclamation material. *Journal of Hazardous Materials* **357**, 63–72. https://doi.org/10.1016/j.jhazmat.2018.05.047.

Liu, H., Hu, G., Basar, I. A., Li, J., Lyczko, N., Nzihou, A. & Eskicioglu, C. 2021 Phosphorus recovery from municipal sludge-derived ash and hydrochar through wet-chemical technology: a review towards sustainable waste management. *Chemical Engineering Journal* **417**, 129300. https://doi.org/10.1016/j.cej.2021.129300.

Ma, P. & Rosen, C. 2021 Land application of sewage sludge incinerator ash for phosphorus recovery: a review. *Chemosphere* **274**, 129609. https://doi.org/10.1016/j.chemosphere.2021.129609.

Ni, M., Pan, Y., Chen, Y., Zhang, X., Huang, Y. & Song, Z. 2021 Effects of seasonal temperature variations on phosphorus removal, recovery, and key metabolic pathways in the suspended biofilm. *Biochemical Engineering Journal* **176**, 108187. https://doi.org/10.1016/j.bej.2021.108187.

Niewersch, C., Battaglia Bloch, A. L., Yüce, S., Melin, T. & Wessling, M. 2014 Nanofiltration for the recovery of phosphorus – development of a mass transport model. *Desalination* **346**, 70–78. https://doi.org/10.1016/j.desal.2014.05.011.

Nzihou, A. & Stanmore, B. 2013 The fate of heavy metals during combustion and gasification of contaminated biomass – a brief review. *Journal of Hazardous Materials* **256–257**, 56–66. https://doi.org/10.1016/j.jhazmat.2013.02.050.

Ottosen, L. M., Kirkelund, G. M. & Jensen, P. E. 2013 Extracting phosphorous from incinerated sewage sludge ash rich in iron or aluminum. *Chemosphere* **91**, 963–969. https://doi.org/10.1016/j.chemosphere.2013.01.101.

Razmjoo, N., Sefidari, H. & Strand, M. 2016 Measurements of temperature and gas composition within the burning bed of wet woody residues in a 4 MW moving grate boiler. *Fuel Processing Technology* **152**, 438–445. https://doi.org/10.1016/j.fuproc.2016.07.011.

Regulation (EU) 2019/1009. Available from: https://eur-lex.europa.eu/legal-content/EN/TXT/?uri=CELEX%3A32019R1009

Shao, J., Yan, R., Chen, H., Yang, H., Lee, D. H. & Liang, D. T. 2008 Emission characteristics of heavy metals and organic pollutants from the combustion of sewage sludge in a fluidized bed combustor. *Energy Fuels* **22**, 2278–2283. https://doi.org/10.1021/ef800002y.

Toledo, J. M., Corella, J. & Corella, L. M. 2005 The partitioning of heavy metals in incineration of sludges and waste in a bubbling fluidized bed. *Journal of Hazardous Materials* **126**, 158–168. https://doi.org/10.1016/j.jhazmat.2005.06.021.

Van de Velden, M., Dewil, R., Baeyens, J., Josson, L. & Lanssens, P. 2008 The distribution of heavy metals during fluidized bed combustion of sludge (FBSC). *Journal of Hazardous Materials* **151**, 96–102. https://doi.org/10.1016/j.jhazmat.2007.05.056.

Wang, Q., Li, J., Tang, P., Fang, L. & Poon, C. S. 2018 Sustainable reclamation of phosphorus from incinerated sewage sludge ash as value-added struvite by chemical extraction, purification and crystallization. *Journal of Cleaner Production* **181**, 717–725. https://doi.org/10.1016/j.jclepro.2018.01.254.

Xu, H., He, P., Gu, W., Wang, G. & Shao, L. 2012 Recovery of phosphorus as struvite from sewage sludge ash. *Journal of Environmental Sciences* **24**, 1533–1538. https://doi.org/10.1016/S1001-0742(11)60969-8.

Yu, X., Nakamura, Y., Otsuka, M., Omori, D. & Haruta, S. 2021 Development of a novel phosphorus recovery system using incinerated sewage sludge ash (ISSA) and phosphorus-selective adsorbent. *Waste Management* **120**, 41–49. https://doi.org/10.1016/j.wasman.2020.11.017.

Zabielska-Adamska, K. 2019 Sewage sludge bottom ash characteristics and potential application in road embankment. *Sustainability* **12**, 39. https://doi.org/10.3390/su12010039.

First received 11 January 2022; accepted in revised form 11 April 2022. Available online 20 April 2022